

Chapter 13

**INORGANIC PIGMENTS TO COLOUR
CERAMIC MATERIALS:
STATE OF THE ART AND FUTURE TRENDS**

Federica Bondioli

Università di Modena e Reggio Emilia
Dipartimento di Ingegneria dei Materiali e dell' Ambiente
Via Vignolese 905, 41100 Modena (I)

ABSTRACT

Inorganic natural and synthetic pigments produced and marketed as fine powders are an integral part of many decorative and protective coatings and are used for the mass coloration of many ceramic materials, including glazes, ceramic bodies, and porcelain enamels. In all these applications, pigments are dispersed (they do not dissolve) in the media, forming a heterogeneous mixture. In conclusion, powders used for colouring ceramics must show thermal and chemical stability at high temperature and must be inert to the action of molten glass (frits or sintering aids). These requirements limit ceramic pigments to a very small number of refractory systems which are fully reacted and relatively inert to the matrix in which they are dispersed. This need for great chemical and thermal stability has dominated research and development in recent years. In this chapter the state of the art will be reported focusing in particular on the specific systems used in this industrial field. The advantages and the limitations of different colours will be underlined with particular emphasis on the current problems and on the possible way to solve them.

INTRODUCTION

Ceramic manufactures have spent the last several years trying to automate repetitive steps, rationalize the production flow and decrease costs without decreasing productivity and production quality. Considerable progress has been made in the development of automated

systems, marking the factory operative 24 hours a day with reduced staff. Studies on how to obtain a better flexibility for the process have resulted in corresponding new developments in kilns, which guarantee faster firing (by 35 to 50 minutes), low energy consumption and optimal quality due to precise vitrification process control and the realization of technology for a continuous production line [1-4]. Conditions for fast firing include the ability to place the products in one layer; a good heat distribution and transfer; the ability to experimentally determine the critical heating rate by carefully monitoring the temperatures of the surface, center and other locations of an actual ceramic product for which the initial firing curve has been designed; the formulation of new, more reactive bodies; the increase of the firing temperatures and the reduction of the particle size to improve the kinetic of the reactions that determine firing; the ability to use more stable glazes based on eutectic compositions; and, finally, the necessity to use more stable coloring solutions. Among all the possible methods of colouring (precipitation, melting of transition metal ions, scattering, etc) the most efficient way, both for technical and economical reasons, to give a ceramic product a stable colouration is still by using pigments introduced inside glazes or bodies before their firing and sintering.

Inorganic natural and synthetic pigments produced and marketed as fine powders are an integral part of many decorative and protective coatings and are used for the mass coloration of many materials, including glazes, ceramic bodies and porcelain enamels.

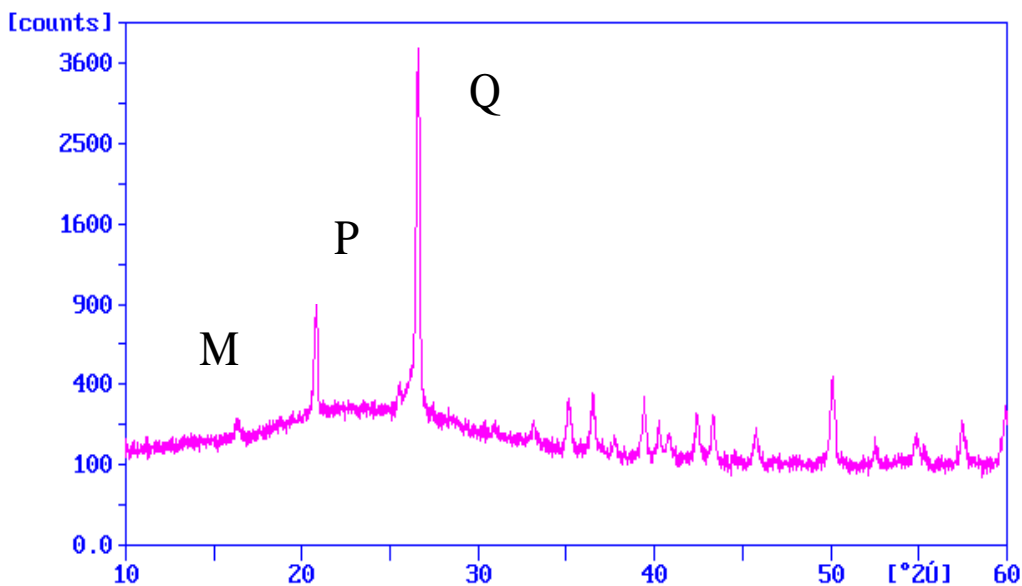


Figure 1. XRD analysis of porcelainized gres coloured with pink $(\text{Cr,Al})_2\text{O}_3$ pigment: characteristic peaks related to pigment structure are visible after firing (Q=quartz; M=mullite; P=pigment)

In all these applications, the pigments are dispersed in the matrix which is to be coloured, forming an heterogeneous mixture. Since they do not have to dissolve in the matrix, one of the most important characteristics of pigments for ceramic materials is their thermal stability at the sinterisation temperature and their chemical stability in respect to the phases, also often

of a fluid nature, that during firing are formed by the action of sinterisation promoters or vitreous frits (Figure 1).

Selecting the right pigments for ceramic decorating requires a basic understanding of pigment characteristics and their reactions with other parts of the production process. Moreover it is rare to be able to find a single pigment that exactly matches the desired color for a given application. Therefore, it is important to understand how to combine colors to give the desired results.

DEFINITION

In general, a pigment is defined as being any solid, organic/inorganic, white, black, coloured or fluorescent that is insoluble in the matrix into which it is incorporated and which does not react chemically or physically with it [5]. By dwelling on pigments in the strict sense of the above definition, only inorganic pigments, containing metallic chromophores as elements of the first transition and rare hearths can be used for the coloration of ceramic materials, both on a large scale as well as being used as an integral part of decorative and protective coatings (glazes).

A classification of ceramic pigment can be done in various way but if we consider how chromophores are incorporated in the base crystalline structure, then it is possible to reach a classification that leads to the distinction of three classes:

- (I) *structural or idiochromatic pigments*: the chromophore is incorporated into the crystalline structure. In this case, therefore, the coloured element is an integral part of the structure as in spinel type pigments, for example CoAl_2O_4 (Figure 2) [6];
- (II) *solid solutions or allochromatic pigments*: the chromophore enters the crystalline structure replacing one of the structural ions; the quantity can vary according to the amount of tonality desired, but, however, it is not stoichiometric. The structure, by itself, is uncoloured but becomes coloured by the introduction, in interstitial or substitutional sites, of chromophoric elements. This is the case of ions V(IV) or Pr(IV) in the ZrSiO_4 crystal that gives, respectively, a blue and a yellow coloration to the white matrix of ZrSiO_4 (Figure 3) [7];
- (III) *inclusion pigments*: coloured oxides that have usually a high instability upon contact with glass, supports or glazes, are made usable through their encapsulation via sinterisation in a vitreous or crystalline matrix, that is extremely stable from a chemical or thermal point of view. Pigments that belong to this class are therefore formed by two, or more, insoluble, phases, that, however, from a colour point of view, act as a single, chromatic unit. The colour does not develop, therefore, by introducing an ion into a crystalline network or by the formation of a solid solution, but rather the crystal which is responsible for colour is occluded in a stable matrix during the process of sinterisation. Examples of this class of pigment are the chromophore molecule $\text{Cd}(\text{S}_x\text{Se}_{1-x})$ and Fe_2O_3 included in a matrix of silicate of zirconium [8-9] or Fe_2O_3 in SiO_2 (Figure 4) [10].

The classification widely used for synthetic inorganic pigments on an international scale is still, however, the American *DCMA (Dry Colour Manufacturers Association)*, that subdivides all crystalline inorganic pigments according to colour, crystallographic class, spectrum of X-ray diffraction and prevailing use. On the basis of this classification, the codes EINECS and CAS were subsequently allocated to each colorant, making the identification of the products easier from a commodity knowledge and toxicological point of view.

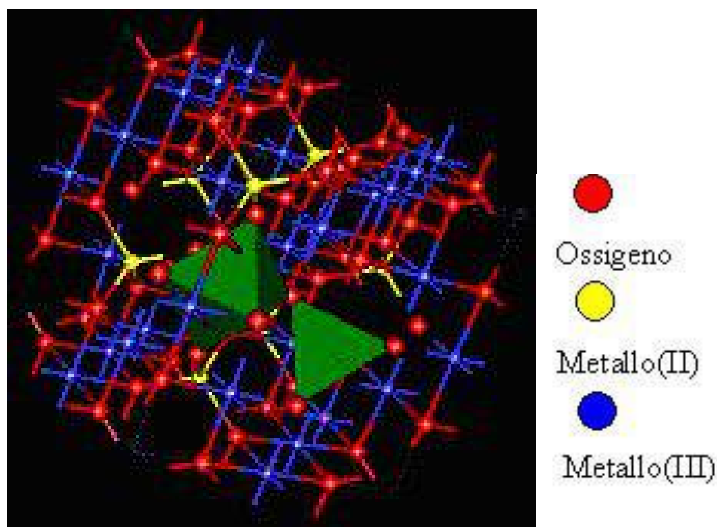


Figure 2. An exemplum of an idiochromatic pigments: cubic spinel structure of CoAl_2O_4

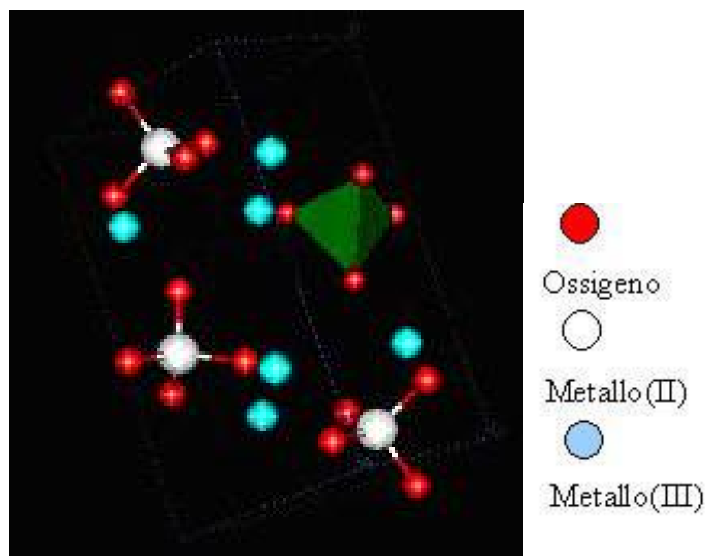


Figure 3. An exemplum of an allochromatic pigment: the zircon structure of $(\text{Zr,Pr})\text{SiO}_4$.

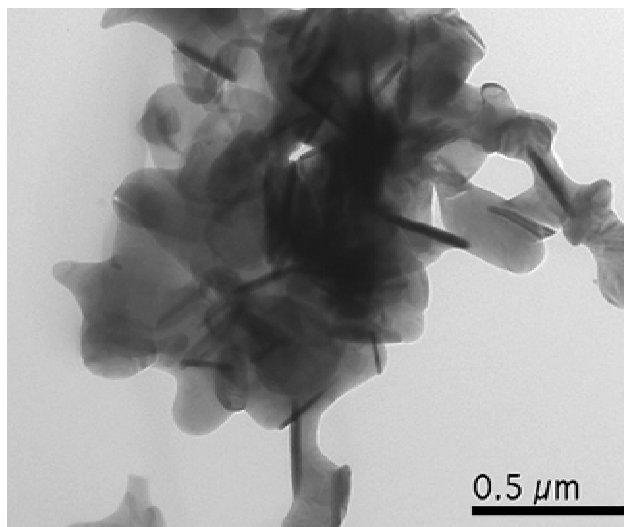


Figure 4. An exemplum of an inclusion pigment: acicular Fe_2O_3 crystals in SiO_2 matrix.

Finally, among all possible methods of classifying inorganic pigments, the one historically used but by no means satisfactory, is that of sub-dividing these pigments into natural and synthetic. Natural pigments are available in nature and for a very long time were the only pigments known and used. For thousands of years, in fact, humankind has beautified its world and expressed its feelings through colour. The first known graffiti date back over 30,000 years to the Palaeolithic: pigments used for colouring the caves at Chauvet-Pont-d'Arc, in South-Eastern France, were black, red and yellow (Figure 5). The pigments based on iron oxides were, and in some cases still are (e.g. the typical red hue of bricks, *brick red*), the most widely used of all the natural pigments. Red, associated with the colour of blood, was indeed the appropriate colour for symbolizing the meaning of life and death. The word "hematite" (the mineral from which many iron-based pigments are derived) comes from the Greek *hema* meaning "blood". Pigments based on iron oxides provided the basic colours for ancient artists, from Egypt to India to China.



Figure 5. Graffiti found in the caves at Chauvet-Pont-d'Arc (France).

Simple natural oxides and spinels are still widely used in industry, displaying excellent colouring properties and being available at a low cost [11]. One of the main drawbacks to their use in mass production is the difficulty in reproducing them if they come from different locations. In fact, they can have a different genesis and, therefore, prove to be poorly homogeneous and generally contain different types and quantities of impurities.

In conclusion, synthetic pigments for ceramic material must show the following characteristics:

- they can be produced at a higher degree of chemical purity and uniformity;
- they can be studied and formulated to obtain colourings that are difficult to obtain using natural inorganic pigments;
- they show greater thermal and chemical stability that allows them to be used in the coloration of materials obtained at high temperatures;
- they are obviously more expensive than natural inorganic pigments since they require different steps of preparation (selection of raw materials at a high level of purity, thermal process of calcination, grinding, quality control, corrections....).

The most common industrial method is based, in fact, on the calcinations of well controlled precursors containing chromophore elements. In such cases, the reaction at the solid state provides for the use of different types and amounts of mineralisers (up to 10% in weight) with the aim of reducing the temperature of synthesis, that varies from 500 to 1400°C according to the system used.

In a ceramic dictionary, mineraliser is a substance that acts in such a way as to lower the temperature of synthesis of the final product and/or promote the sinterisation. In the field of pigments, these substances can essentially be subdivided into two classes:

1. *promoting mineralisers*: increase the solid state reactivity by the formation of a fluid phase (molybdates, borates, halogenides), by the formation of a volatile phase (fluorures with pigments containing silica), by superficial activation or through the control and stabilisation of the oxidation conditions (nitrates);
2. *structural mineralisers*: are those that contain ions that are capable of structurally integrating themselves in the pigment crystal structure producing a cell distortion. This change can cause either an increase in the solubility of the chromophore or a modification of the intensity of the crystalline field on the ion and therefore, leading to a variation in the coloration of the structure.

For exemplum the formation mechanism of praseodymium-doped zircon [12], a market leader ceramic pigment in the high temperature color range, were defined in presence of mineralizers as a two steps mechanism. At lower temperature (Figure 6a), the silicate formation is facilitate by a viscous phase, which is constituted by the mixture of mineralizers (NaF and NaCl mixture which melts at 726°C), while increasing temperature, the reaction occurs between SiO₂ and mineralizers to produce a volatile halide (SiX₄, where X is a halide element) that successively reacts with ZrO₂ and praseodymium oxide (Pr₆O₁₁) at the ZrO₂ sites (Figure 6b).

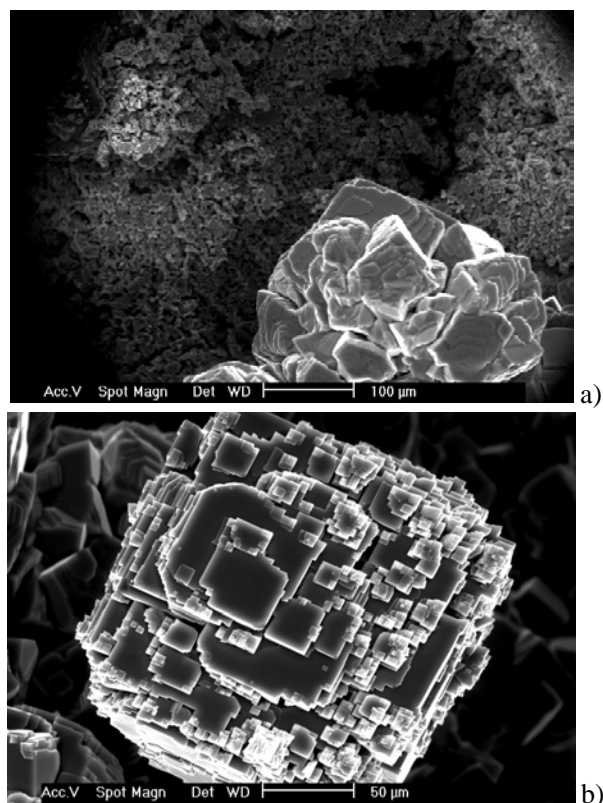


Figure 6. Reaction mechanism of $(\text{Zr,Pr})\text{SiO}_4$ yellow pigment formation determined by ESEM analysis at high temperature. 866 (a) and 900°C (b).

The role of mineralizers in the solid state synthesis to promote or induce selectively the formation of certain species is not however well understood. As a matter of fact different mineralizers seem to have different effects and in many case more than one mechanism is involved in their action. Is therefore necessary to examine processes that occur at very high and wide temperature range.

PIGMENT PROPERTIES AND APPLICATIONS

Aside from the pigment's structure and classification, the value of a ceramic pigment result from its physical-optical properties. These are primarily determined by pigments crystal structure, physical characteristics (particle size and distribution, particle shape, agglomeration, etc.) and chemical properties (composition, purity, stability, etc.). However, the two most important physical-optical properties of pigments to be considered are the ability to color the environment in which they are dispersed and to make it opaque.

Otherwise, a significant limitation on the selection of ceramic pigments is the predefinition of processing parameters imposed during coating application and firing. An engobe or body stain must be stable during tile firing, usually between 1200-1300°C. An underglaze color, or a coloured glaze, must be stable during glost firing, usually between

1000-1200°C, and to corrosion by molten glaze ingredients. An overglaze or glass color needs to be stable during decorative firing applied to it, usually between 625-775°C. A more important factor here is corrosion by the molten flux in the application (generally lead oxides).

Physical Properties

Particle size and particle size distribution are the most fundamental measured properties of powders. Those properties impact a number of ceramic pigment characteristics. Those affected the most are color, color strength and rheological properties. For inorganic pigments to be useful in most applications, they must have an average particle size between 0.1 and 10 μm . Selecting an optimum particle size distribution is a compromise between considerations of dissolution rate, agglomeration of the pigment, loss of strength on milling, uneven surface smoothness and pigment strength. The optimum particle size is the largest size that gives adequate dispersion and adequate strength in letdowns.

Optical Properties

The opacity of a pigment lies in its ability to prevent the transmission of light through the medium. The opacity of a pigments is a function of the pigment particle size and of the difference between the pigments refractive index and that of the media in which the pigment particles are dispersed.

For ceramic pigments to be effective as scattering, the discrete substance must have a refractive index that differs appreciably from that of the glassy phase, because the greater the difference in refraction index between the matrix and the scattering phase, the greater the degree of opacity. Because generally the refraction index of glazes is 1.5-1.6, the refraction index of opacifiers must be significantly higher or lower of this value. Some possibilities are reported in Table I. In the opacifier choice are important also other factors; i.e. titanium dioxide, in the anatase form, has a very high refraction index and is the most used for applications below 1000°C. At around 850°C, in fact, anatase transforms in rutile that absorbs in the visible region developing a cream color.

Regarding the particle size, a pigment with particles size approaching that of the wavelength of light provides the maximum scattering of light. However, excessive fineness leads to increase the solubility in the glaze and glassy phases and difficulties in dispersion.

The pigment color is uniquely described by its spectral reflectance curve (Figure 7). This curve shows the fraction of light reflected at each wavelength from a material. Obviously, the colour of an object is entirely characterised by its spectral behaviour, that is from knowing which wavelengths of light it absorbs, which it reflects and which it diffuses. It is not practical, however, that every time one wants to characterise or reproduce a colour, one has to measure and refer to the spectral-photometric curves on graphs, or rather the transmission and reflection in all its visible ranges.

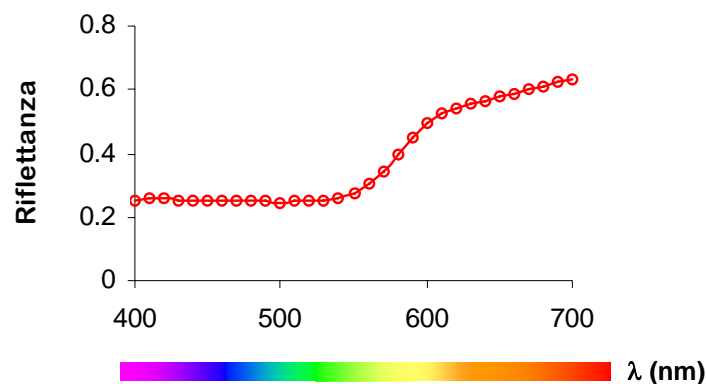


Figure 7. The reflectance curve of a red pigment.

In the industrial practice, however, to exclude the particular conditions of illumination and the physio-psychological response of the observer, a color is defined using the CIELab method (L^*, a^*, b^* system) that measures the absorption intensity in the visible [13]. The formulation, as well as the adjustment of glazes color in the ceramic tile industry, however, is still empirical, making its control difficult. Moreover a common problem is the hue variation between the products that not only impairs the product appearance but also increases stock management costs, and is prejudicial to product competitiveness. This hue variations can be caused by process variables as i.e. pigment and opacifier preparation conditions that affect the pigments and opacifiers physical and chemical properties.

The control of these color problems is generally made using the CIELab system, through the measure of L^* , a^* , b^* parameters, obtained by the analysis of the reflectance curves provided by a spectrophotometer. But despite this system have some limitations. In fact there isn't a systematic relation between the L^* , a^* , b^* values and the concentration of added pigments. The L^*, a^*, b^* coordinates of glazes prepared with different percentages of black pigment (spinel Ni-Fe-Cr) and opacifier ($ZrSiO_4$) are showed in Figure 8 [14]. The L^* parameter (lightness) reduces as the pigment concentration is increased, as expected due to the major quantity of particles pigment that absorbs the light. The a^* and b^* parameters, instead, have aleatoric changes with difficult interpretation underlining the difficulty to use these parameters for the formulations of colors.

The model developed by Kubelka-Munk (1931) [15] supported in reflectance data can be instead very helpful to explain the color variation. This model relates the reflectance (R) for every wavelength to the absorption (K) and scattering (S) of light by pigment particles. This means that for every frequency of the visible spectrum, every component of a formulation possesses a coefficient of absorption, K , and a coefficient of scatter, S . In particular, when the layer of the absorbing scattering material is so thick that no light penetrates through the layer (opaque surfaces), the relationship described the Kubelka–Munk theory, taking into account also the Saunderson correction [16], is given by:

$$\frac{K_{\lambda}}{S_{\lambda}} = \frac{(1 - r_{\lambda})^2}{2r_{\lambda}} \quad (1)$$

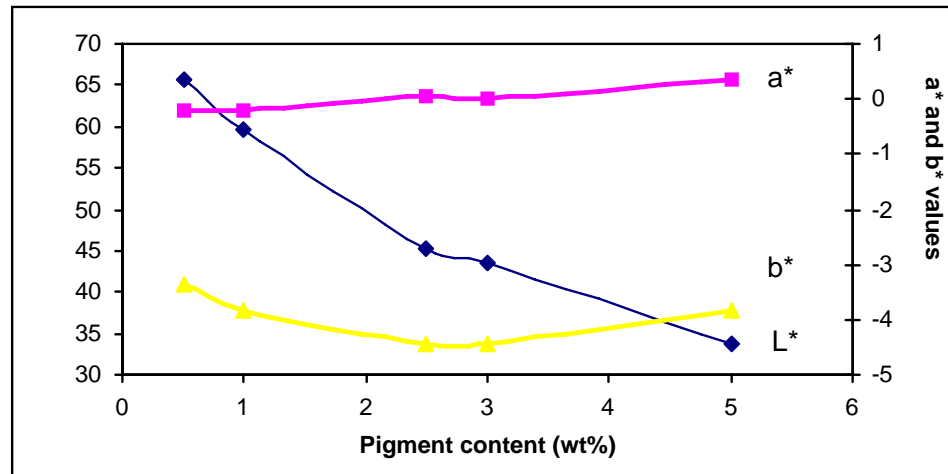


Figure 8. L*, a*, b* parameters as a function of the percentage of black pigment (spinel Ni-Fe-Cr) in the glazes.

where r_λ is the decimal fractional reflectance ($0 < r < 1$) measured at the wavelength λ with the specular component excluded. Another important equation for color matching, developed by Duncan [17], demonstrates the additivity in a mixture M of the absorption and diffusion contributions of each component:

$$\frac{K_\lambda}{S_\lambda} = \frac{\sum c_n K_{n(\lambda)}}{\sum c_n S_{n(\lambda)}} \quad (2)$$

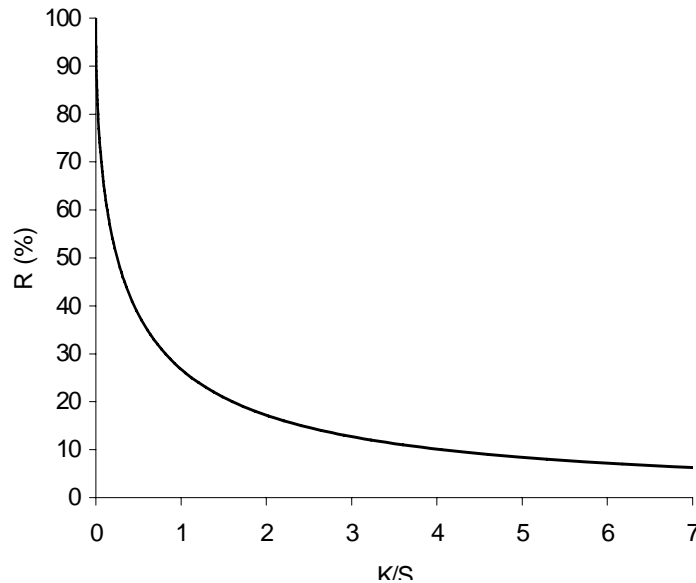


Figure 9. Graph showing the relationship of reflectance, R_∞ , and the ratio K/S according to Eq 1. [Patton, 1973]

where c_n is the fractional concentration ($0 < c_n < 1$) of the n th pigment in the mixture; $K_n(\lambda)$ the absorption coefficient of the n -th pigment in the mixture at the wavelength λ ; and $S_n(\lambda)$ the scattering coefficient of the n -th pigment in the mixture at the wavelength λ . To make use of this theory, one needs a straightforward way to obtain these coefficients from measurable reflectance data. In particular knowing these coefficients for all the components of a mixture it is possible to obtain the reflectance value, and thus the color, that it can be developed by a mixture, changing the components concentration. In fact:



$$(3)$$

where for the Saunderson correction for an opaque glaze surface, $R_\lambda = r_\lambda / (0.576 + 0.4r_\lambda)$ with r_λ decimal fractional reflectance ($0 < r < 1$) measured at the wavelength λ with the specular component excluded.

The simple equation 1 tells that if the absorption, K , is increased and the scattering, S , is kept constant, the reflectance is decreased. Thus adding a strongly absorbing pigment, such as black, to a system its reflectance decreases; while if S is increased keeping K constant, the reflectance is increased. Thus adding a strongly scattering pigment, such as white, to a system the reflectance increases; if both the absorption and scattering are changed by the same quantity, this will not affect the resulting reflectance or the color (Figure 9). Thus changing the amount of pigment in a system the reflectance does not change when hiding is complete. Remembering that the nature of the color is described by its spectrophotometric curve and that at each wavelength the Kubelka-Munk model describes how the reflectance is determined, one can visualize how the curve may be modified in a desired way.

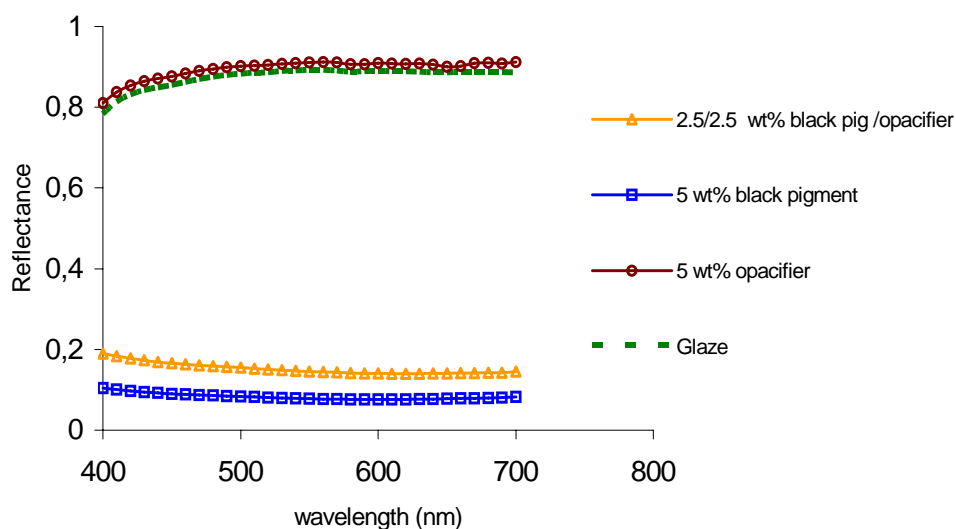


Figure 10. Reflectance curves of the four glazes samples prepared to calculate the Kubelka-Munk coefficients.

In the spinel black pigment exemplum, from equation 1 and with the reflectance curves of the prepared glazes (Figure 10) is possible to calculate the values of the K/S (absorption light caused for the pigment) at each wavelength of visible region as a function of the concentration of pigment added (Figure 11). The Figure shows that the K/S value increases as the quantity of the pigment is increased with a small exponential tendency starting from 3.0% of pigment. This indicate that with the Kubelka-Munk model is possible to relate systematically the color with the quantity of pigment added.

The reflectance curves predict by Kubelka-Munk model are showed in Figure 12. An excellent agreement between the experimental curves and the model curves was observed. The deviations are lesser that 2.0%.

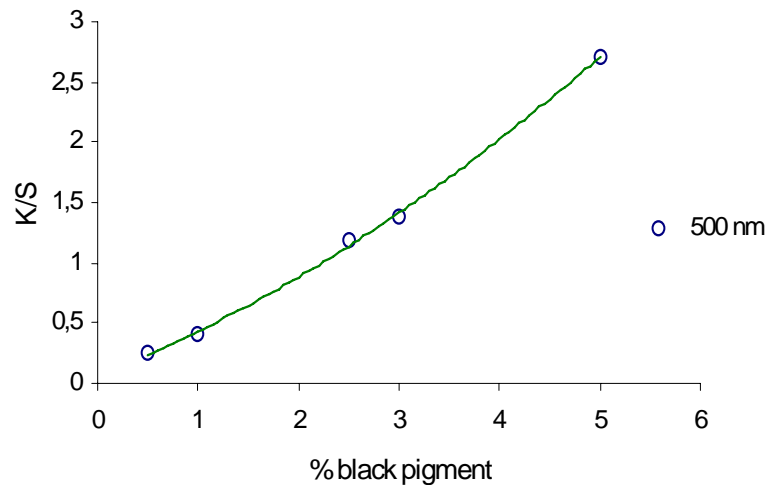


Figure 11. Kubelka-Munk absorption as a function of the black pigment (spinel Ni-Fe-Cr) concentration in the glaze.

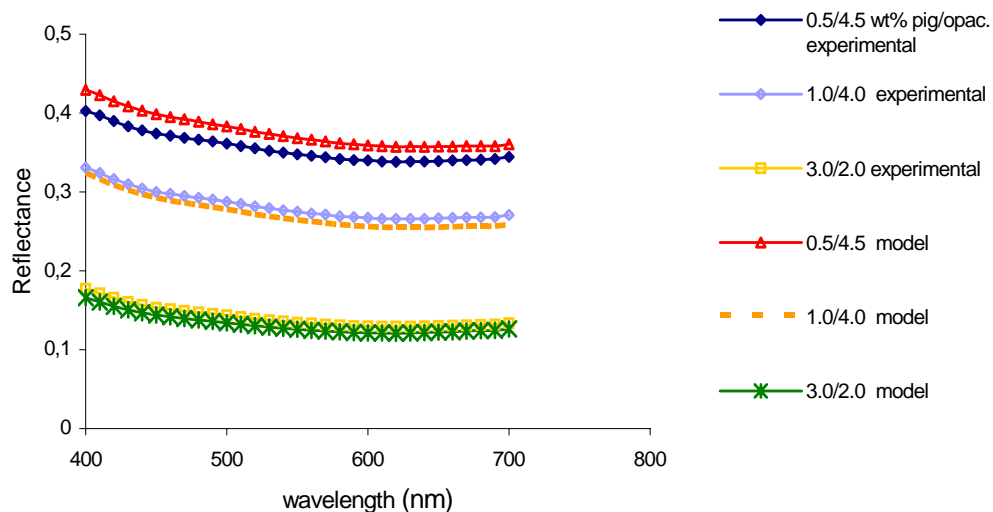


Figure 12. Reflectance curves obtained experimentally in comparison with that determined by the Kubelka-Munk model for same glazes prepared.

Algorithms in the formulation of colors is not a new idea in the industry [18-21]. It has been approximately 50 years since the first colorant formulation algorithm was reported introducing the color matching concept. With color matching, we mean the ability to reproduce, through mixing few fundamental pigments, whatever type of color experimentally measured by using algorithms of calculus. In activities such as printing, the textile industry, plastics or cold paints, this technique represents a working tool, long consolidated and efficient in supplying rapid solutions to many of the chromatic problems of the production process, both those of a formulating and qualitative nature. The advantages are a lot: the possibility to have an elevated number of colors using a low number of pigments; the rejects elimination in the pigment production because the color matching equipment can prepare in real time the required volume of mixtures; the possibility to replicate colors also if it is not available the pigment with the target color; the possibility to adjust errors in the preparation of the color; etc. These aspects should be certainly advantageous also in the ceramic field where many producers now use different typology of applicators (flat, drum, rotary with photoincisive rollers serigraphic machines, ink jet printing) that, in many plants, frequently cohabit. All these factors normally leads to use a wide range of decorating materials (often a question of hundreds of colored products) that make up a complex system to manage both at a warehouse and production level. However, despite various attempts (studies intended to predict the color of a ceramic glaze can be found with interesting results in literature), in ceramic tiles sector the technology of colorant formulation via software has not found a fertile field. For the final result, in fact, some specific limitations, characteristics of a ceramic material that develops its color during firing, have to be considered. The most important is connected with the thermal and chemical stability that pigments must have towards the molten glass (frits or sintering aids) developed during the firing cycle at high temperatures: the same pigment, in fact, can develop slightly different colors depending on both firing temperature and chemical composition of glaze or ceramic body to color. Aspects such as the grain size distribution, the chemical and physical interaction between pigments and glazes, variations during the firing process, the final appearance of the ceramic tile surface, make up a series of elements that influence in a determining way not easily controllable the development of colors. All the most modern formulation softwares are essentially based on the application of the Kubelka–Munk theory, the most widely used in industrial sectors, in the form used for opaque surface coatings. However, in order to determine the coefficient of absorption, K , and the coefficient of scatter, S , for all the components in a mixture it is necessary to introduce a series of approximations.

Artificial neural networks (ANN) are computational models based on biological neural networks. They can be used to represent complex relationships between inputs and outputs or to find patterns in data. ANN are applied within a large number of cases, both in science and industrial fields, thank to their highly mathematical flexibility. The models can be used to carry out simulation in a very quickly and inexpensive way. Finally, they can be used to optimize one or more independent parameters in the same time so reducing costs in a very efficient way, if the model was correctly built. Samples were prepared using thirty industrial pigments and one frit for wall tiles. Mixing the pigments, seventy nine samples were prepared in a fast ball mill and applied as water suspension on fired wall tiles. After drying, the samples were fired in an industrial firing cycle. The color data were analyzed using the open source software JOONE (Java Object Oriented Neural Engine) [22], in order to verify if ANN is an available method to carry out colour matching in ceramic tile production. Efficiency of a

neural network architecture depends by a number of factors. Among the most important ones: architecture of the network; number of hidden layer; number of neurons for each hidden layer; number of epochs; activation function used; learning parameters etc. The validity is restricted to the conditions used to produce the experimental data. When the fixed parameter are changed, the network is not able to predict the right mix of pigments, but if they are respected the results are very interesting. A important advantage is the possibility to avoid the time consuming step of determination of K and S parameters in Kubelka-Munk method, because of it is possible to use directly the data obtainable by the production database to built the neural model.

Chemical Reactivities

Selecting the right pigments for ceramic decoration requires a basic understanding of pigment characteristics and their reactivity with other constituents of the ceramic material.

The most important glaze consideration is probably the presence or absence of ZnO in the glaze. The pink $(Al,Mn)_2O_3$, green-black $(Fe,Cr)_2O_3$, Victoria-green garnet, orchid chrome-tin cassiterite and pink chrome-tin sphene are not stable in the presence of zinc oxide mainly due to the formation of spinels. The brown iron ematite, pink chrome-alumina spinel, brown iron-chromite spinel, brown zinc-ferrite spinel and brown zinc-iron chromite spinel requie high ZnO concentration. High calciumoxide concentration is required for adequate stability of Victoria-green carnet and chrome-tin splene. CaO should be avoided when using pink chrome-alimuna spinel, brown zinc-ferrite spinel and brown zinc-iron-chromite spinel. Pigments containing chromium(III) oxide are incompatibile with pigments containing tin oxide.

The presence or absence of PbO in a glaze affects some pigments. Victoria-green and cobalt-black pigments are stronger in a high PbO glaze. Blue zircon-vanadium, yellow zircon-praseodymium and pink gray zircon pigments are stronger in low PbO and lead-free glazes.

FUTURE TREND

To contribute to the innovation process in the traditional ceramic field and to maintain a high level of competitiveness and market penetration, the research has to be directed to both the transfer and the application of the scientific knowledge to the industrial practice. This has to be realized by means of the critical revision of the different production steps allowing the design, realization, development and industrial application of new materials, essentially of ceramic or glassy nature, with higher aesthetical and functional performances.

A strong distinctive element of the scientific and technological development of the last ten years is represented by the increasing interest and by the remarkable research dedicated to nanomaterials. In fact it has been observed that, when a material is constituted by nanometric component, different properties, interesting from a technological point of view, are also considerably changed with respect to the materials science laws. This evidence starts up the development of completely innovative materials and applications. This is therefore an area

that, using a multidisciplinary approach, looks to revolutionize all the most important technological and productive fields.

The most important exemplum is the application of innovative technology solutions such as the digital printing to the ceramic field. The research is mainly devoted to the optimisation of the ink-jet printer for ceramic tiles already present on the market but also to the formulation of specific ceramic inks. In fact, the emerging field of digital printing onto ceramic bodies requires a four color set of pigments to produce process color. The way to obtain such colors are different but the research is mainly devoted to innovative nanosized pigments with improved aesthetical properties. The objective is pursued through the development of synthesis methods capable to limit or eliminate the problems belonging to this specific technology when applied to the ceramic industrial process, i.e. high wear of the printing heads. From these considerations the optimal solution of these problems can be identified in the nanopowders technology allowing to obtain the complete range of colour with the right hue and grain size distribution narrower with respect to the micro powders.

Is thus clear that the correct running of the synthesis method and the knowledge of the parameters that influence the dimensions, the grain size distributions and the morphologies of nanoparticles become strategically important. There are a very high number of production techniques to obtain nanostructured powders. In particular, two approaches can be individualized:

- Top down that is based on the successively granulometric refinement of a micrometric powder mainly by milling, lithography or etching;
- Bottom up. In this field the methods can be subdivided in three categories:
 - condensation from vapour phase;
 - wet chemical methods (Figure 13);
 - solid state process.

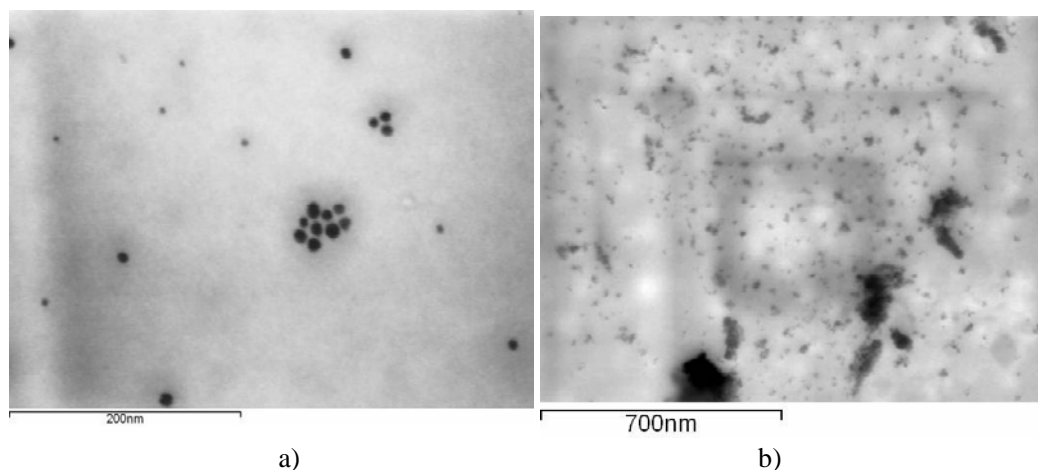


Figure 13. Exempla of powders obtained by chemical method (microgrphas courtesely given by Colorobbia Italia, ParNaSos Products: Au particle (a); titania particle (b))

The nanostructured pigments are characterized by a high thermal and chemical stability. In Figure 14 the mineralogical analysis on a Co-blu pigment both with a micro and nano grain size distribution. While the MICRO pigment was obtained by solid state reaction generally starting from Co_3O_4 and $\text{Al}(\text{OH})_3$, the NANO pigment was obtained by condensation from vapour phase. Mineralogically both the pigments are constituted by CoAl_2O_4 (ICDD #00-003-0896) with the spinel general formula AB_2O_4 . The NANO pigment has a minor crystallinity as underlined by both the lower peak intensity and the higher peak broadening. To evaluate the thermal and chemical stability, the NANO pigment were mixed (2 wt%) with two commercial frits for high temperature (a transparent gloss and a white gloss respectively) and the obtained mixture studied by a heating optical microscope. The obtained results show the stability of the nanoparticles in the used frits (Figure 15-17).

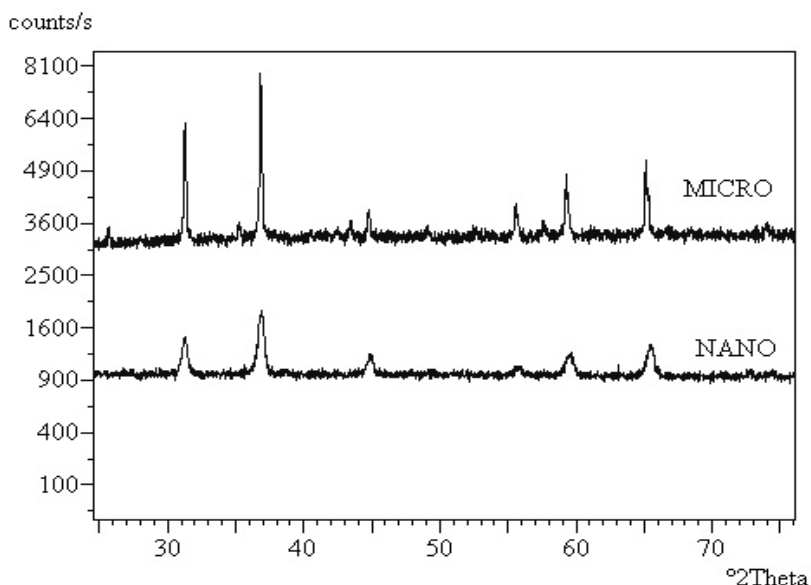


Figure 14. X-ray diffraction patterns of both NANO and MICRO Co-blu pigment.



Figure 15. Stability of the CoAl_2O_4 nanoparticles in two commercial frits for high temperature.

REFERENCES

- [1] Proven, A. *Interceram*, 1990, 39[7], 39-44.
- [2] Schoppe, K.H. *Interceram*, 1990, 39[3], 17-22.
- [3] Avallone, A. *Interceram*, 1995, 44[3], 186-188.
- [4] Sladek, R. *Interceram*, 1995, 44[3], 176-179.
- [5] *Pigment Handbook*, Ed. by P.A. Lewis, J. Wiley & Sons, New York, Vol. 1, p. VII (1988).
- [6] Ferrari, A.M.; Leonelli, C.; Manfredini, T.; Miselli, P.; Monari, G.; Pellacani, G.C. In *Advances in Science and Technology 3A*; Vincenzini, P.; Ed.; Techna: Faenza, IT; 1995; pp 83-90.
- [7] Eppler, R.A. *Am. Ceram. Soc. Bull.* 1987, 56[2], 213-217.
- [8] Lambies, V.; Rincòn, J.M. *Trans. J. Br. Ceram Soc.* 1981, 80, 105-108.
- [9] Berry, F.J.; Eadon, D.; Holloway, J.; Smart, L.E.; *J. Mat. Sci.* 1999, 34, 3631-38.
- [10] Bondioli, F.; Ferrari, A.M.; Leonelli, C.; Manfredini, T. *Mat. Res. Bull.* 1998, 33[5], 723-729.
- [11] Bondioli, F.; Ferrari, A.M.; Leonelli, C.; Manfredini, T. *Ceram. Eng. Sci. Proc.* 1997, 18[2], 44-58.
- [12] Bondioli, F.; Corradi, A.; Ferrari, A.M.; Manfredini, T.; Baldi, G. *J. Am. Ceram. Soc.* 2000, 83[6], 1518-1520.
- [13] Johnston, R.M. in *Pigment Handbook*; Putton. T.C.; Ed.; Wiley-Interscience Publication; New York (NY) 1973; Vol. 3, pp 229-88.
- [14] Schabbach, L.M.; Bondiola, F.; Ferrari, A.M.; Manfredini, T.; Setter, C.O.; Fredel, M.C. *J. Euro. Ceram. Soc.* 2007, 27, 179-184.
- [15] Kubelka P., Munk F., Ein Beitrag zur Optik der Farbanstriche, *Z. Tech. Phys.* 1931, 12, 593-601.
- [16] Saunderson, J.L. *J. Opt. Soc. Am.*, 1942, 32[12], 727-732.
- [17] Duncan, D.R. *J. Oil Colour Chem. Assoc.*, 1962, 45, 300-304.
- [18] Murdock, S.H.; Wise, T.D.; Eppler, R.A. *Am. Ceram. Soc. Bull.*, 1990, 69[2], 228-231.
- [19] Murdock, S.H.; Wise, T.D.; Eppler, R.A. *Ceram. Eng. Sci. Proc.* 1990, 11[3-4], 270-277.
- [20] Eppler, D.R.; Eppler, R.A. *Cer. Eng. Sci. Proc.*, 1998, 19[2], 17-22.
- [21] Bondioli, F.; Manfredini, T.; Romagnoli, M. *J. Euro. Ceram. Soc.*, 2006, 26[3], 311-316.
- [22] Available at <http://www.joone.org>

Chapter 14

**SYNTHESIS AND CHARACTERIZATION
OF SEVERAL SERIES OF
SUBSTITUTED METALLOPHthalOCYANINES**

Fangdi Cong^{a,b}, Xiguang Du^{a,b,}, Jianxin Li^a,
Dongliang Tian^b and Wenjuan Duan^b*

^aCollege of Material Science & Engineering, Nanjing University of Aeronautics and
Astronautics, Nanjing, Jiangsu, 210016, China

^bFaculty of Chemistry, Northeast Normal University, Changchun 130024, China

ABSTRACT

The twenty-four substituted metallophthalocyanines were synthesized, in two steps, from 4-nitrophthalonitrile or 3-nitrophthalonitrile, and characterized by MS, ¹H NMR, UV-vis, IR and element analysis. The results showed that they all were consistent with proposed structures. They behaved excellent solubility in some organic solvents, but the stability of them in solution was not good as in solid state. According to the scopes of red shift, the impact of metals, substituents and substitution positions on Q-bands could be displayed as follow: Mn > Zn ≈ Cu > Ni ≈ Co; 2-isopropyl-5-methylphenoxy ≥ 4-tert-butylphenoxy ≥ quinolin-8-yloxy ≥ 2-methoxyethoxy; non-periphery > periphery. The research displayed that the alternative ways to control the Q bands of Pc compounds to have a big change were to alter the chemical value of metal in the center of Pc ring, replace the atom banding directly with Pc ring or its chemical circumstance, and change the substitution position of substituent on Pc ring (periphery or non-periphery).

Key words: Phthalocyanine, Synthesis, UV-vis spectra, Q band, solubility, stability

* Corresponding author: Tel: +86-0431-85098720; E-mail: xgdu@yahoo.cn

1. INTRODUCTION

Pc compounds have extensive applications in the area of material science, such as liquid crystal [1], catalysis [2], nonlinear optics [3], Photodynamic therapy [4], film [5] and semiconductor [6], etc. The various functions are associated with their aromatic 18- π electron system [7], which cause them all have the special Q band absorption (around 700 nm). So almost of all the investigations on Pcs were paid attention to the properties [8] and changes [9] of Q bands, which might present the significant information implying the potential application of Pcs.

In order to obtain more spectral data of Pc complexes, a number of substituted metal and metal-free Pcs were synthesized by diversified methods [10-12]. But many Pc compounds were practically insoluble in common organic solvents due to the intermolecular interactions between the macrocycles, which limited the investigations on them as well as the applications of them [13]. Hence a considerable effort was made to generate novel soluble substituted Pcs by introduction of the suitable substituents on the periphery that, to some extent, increases the distance of 18- π electron conjugated systems of Pcs and facilitates the solubility [14,15].

In our previous works on the synthesis of soluble substituted Pc compounds [16-18], we prepared some Pc derivatives with enhanced solubility in common organic solvents, which derived from the steric bulk and solvent affinity of the substituents preventing aggregation [19]. We also found that the coordinated metals in the center of Pc ring, substituents around Pc ring and substitution positions (periphery and non-periphery) had different impacts on the UV-vis of Pcs [20,21]. In order to systemically understand the impact of above three factors on UV-vis spectra, a series of soluble substituted metal Pcs, $1a_1\sim 1e_4$ and $2a_1\sim 2b_2$, were synthesized according to the modified strategy based on the literature [16]. The orders of Q-band wavelength derived from different metals, substituents and substitution positions were obtained, respectively. The potential ways to availably change the Q-band wavelength were suggested in this paper.

2. EXPERIMENTAL

2.1. Materials and Methods

Pentan-1-ol was distilled from Na prior to use. DMSO was predried over BaO and distilled under reduced pressure. Column chromatography purifications were performed on silica gel. All other reagents and solvents are commercial available and used without further purification. Petroleum ether used had bp 60–90 °C.

^1H NMR spectra were recorded on a Bruker AV 500 spectrometer. IR spectra were measured on a Magna 560 FT-IR spectrometer. UV/Vis spectra were taken on a Cary 500 UV-VIS-NIR spectrophotometer. MS spectra were obtained on a LDI-1700-TOF mass spectrometer. Elemental analyses were performed on a Perkin-Elmer 2400 Elemental Analyzer.

2.2. Synthesis of Several Substrates

4-(2-isopropyl-5-methylphenoxy)phthalonitrile; typical procedure:

4-nitrophthalonitrile (6.92 g, 40.0 mmol) and 2-isopropyl-5-methylphenol (6.00g, 40.0 mmol) was added to 80 mL DMSO at r.t. The reaction mixture was stirred and LiOH (2.4 g, 100 mmol) was added over 2 h, and then the mixture was stirred for 2 days. The reaction progress was monitored by TLC analysis. The mixture was then poured into 10% NaCl (400 mL). The product was collected by vacuum filtration. The crude product was purified by column chromatography with petroleum ether–anhyd Et₂O (1:1) as the mobile phase to afford yellow crystal of 4-(2-isopropyl-5-methylphenoxy)phthalonitrile; yield: 9.88 g (89%), m.p. 106~108°C. ¹H NMR (500 MHz, CDCl₃) δ = 7.708 (d, 1 H, *J* = 8.5 Hz, ArH), 7.295 (d, 1 H, *J* = 8.5 Hz, ArH), 7.219 (s, 1 H, ArH), 7.189 (d, 1 H, *J* = 8 Hz, ArH), 7.109 (d, 1 H, *J* = 8 Hz, ArH), 6.745 (s, 1 H, ArH), 2.958 (m, 1 H CH), 2.331 (s, 3 H, ArCH₃), 1.154 (d, 6 H, *J* = 6.5 Hz, CH(CH₃)₂). MS (QUSTAR-TOF): *m/z* calcd for [M]: 276.1; found: 299.1 (an isotopic cluster peak) [M +Na⁺], 314.9 (an isotopic cluster peak) [M +K⁺]. UV/Vis (CHCl₃): λ_{max} = 264, 306 nm. IR (KBr): 2230 cm⁻¹ (C≡N), 1246 cm⁻¹ (C-O-C).

4-(4-tert-butylphenoxy)phthalonitrile

Yellow solid; yield: 10.20 g (92%), m.p. 116~118°C. ¹H NMR (500 MHz CDCl₃): δ = 7.711 (d, 1 H, *J* = 2 Hz, ArH), 7.477 (d, 1 H, *J* = 2 Hz, ArH), 7.464 (s, 1 H, ArH), 7.248 (q, 2 H, *J* = 2 Hz, ArH), 6.994 (q, 2 H, *J* = 2 Hz, ArH), 1.358 (s, 9 H, t-C₄H₉). MS (QUSTAR-TOF): *m/z* calcd for [M]: 276.1; found: 299.1 (an isotopic cluster peak) [M +Na⁺], 314.9 (an isotopic cluster peak) [M +K⁺]. UV/Vis (CHCl₃): λ_{max} = 264, 306 nm. IR (KBr): 2231 cm⁻¹ (C≡N), 1244 cm⁻¹ (C-O-C).

4-(quinolin-8-yloxy)phthalonitrile

White solid; yield: 8.78 g (81%). m.p. 176~178°C. ¹H NMR (500MHz, CDCl₃): δ = 9.031 (d, 1 H, ArH), 8.504 (d, 1 H, ArH), 7.925 (d, 1 H, ArH), 7.722 (m, 3 H, ArH), 7.584 (d, 1 H, ArH), 7.225 (d, 2 H, ArH). MS (QUSTAR-TOF): *m/z* calcd for [M]: 273.0; found: 271.8 (an isotopic cluster peak) [M +Na⁺]. UV/Vis (CHCl₃): λ_{max} = 263, 296 nm. IR (KBr): 2230 cm⁻¹ (C≡N), 1246 cm⁻¹ (C-O-C).

4-(2-methoxyethoxy)phthalonitrile

Yellow solid; yield: 6.63 g (82%). m.p. 80~82°C. ¹H NMR (500MHz, CDCl₃): δ = 7.711 (dd, 1 H, *J* = 8.7 Hz, ArH), 7.309 (d, 1 H, *J* = 2.52 Hz, ArH), 7.239 (m, 1 H, *J* = 8.8 Hz, ArH), 4.217 (m, 2 H, ArOCH₂), 3.784 (m, 2 H, CH₂O), 3.449 (s, 3 H, OCH₃). MS (QUSTAR-TOF): *m/z* calcd for [M]: 202.1; found: 225.4 (an isotopic cluster peak) [M +Na⁺]. UV/Vis (CHCl₃): λ_{max} = 264, 297, 305 nm. IR (KBr): 2230 cm⁻¹ (C≡N), 1240 cm⁻¹ (C-O-C).

3-(2-isopropyl-5-methylphenoxy)phthalonitrile and 3-(4-tert-butylphenoxy)phthalonitrile can be obtained by the similar sythesis method after 4-nitrophthalonitrile was replaced with 3-nitrophthalonitrile.

3-(2-isopropyl-5-methylphenoxy)phthalonitrile

Yellow solid; yield: 9.18 g (83%). m.p. 84~86°C. ¹H NMR (500 MHz, CDCl₃): δ = 7.543 (dd, 1 H, *J* = 8 Hz, ArH), 7.425 (d, 1 H, *J* = 8 Hz, ArH), 7.286 (d, 1 H, *J* = 8 Hz, ArH), 7.091 (d, 1 H, *J* = 9 Hz, ArH), 6.971 (d, 1 H, *J* = 9 Hz, ArH), 6.769 (s, 1 H, ArH), 3.023 (m, 1 H, CH), 2.320 (s, 3 H, ArCH₃), 1.182 (d, 6 H, *J* = 6.5 Hz, CH(CH₃)₂). MS (QUSTAR-TOF): *m/z* calcd for [M]: 276.1; found: 299.1 (an isotopic cluster peak) [M +Na⁺], 314.9 (an isotopic cluster peak) [M +K⁺]. UV/Vis (CHCl₃): λ_{max} = 219, 321 nm. IR (KBr): 2233 cm⁻¹ (C≡N), 1240 cm⁻¹ (C-O-C).

3-(4-tert-butylphenoxy)phthalonitrile

Yellow solid; yield: 9.52g (86%). m.p. 104~106°C. ^1H NMR (500 MHz, CDCl_3): δ = 7.551 (dd, 1 H, J = 8 Hz, ArH), 7.451 (d, 2 H, J = 9 Hz, ArH), 7.427 (d, 1 H, J = 8 Hz, ArH), 7.093 (d, 1 H, J = 8 Hz, ArH), 7.022 (d, 2 H, J = 9 Hz, ArH), 1.342 (s, 9 H, t- C_4H_9). MS (QUSTAR-TOF): m/z calcd for [M]: 276.1; found: 299.1 (an isotopic cluster peak) $[\text{M} + \text{Na}^+]$, 314.9 (an isotopic cluster peak) $[\text{M} + \text{K}^+]$. UV/Vis (CHCl_3): λ_{max} = 214, 321 nm. IR (KBr): 2235 cm^{-1} ($\text{C}\equiv\text{N}$), 1247 cm^{-1} (C-O-C).

2.3. Synthesis of MPcs 1a₁~1e₄ and 2a₁~2b₂

Synthesis of 1a₁; typical procedure: 4-(2-isopropyl-5-methylphenoxy)phthalonitrile (1.04 g, 4.0 mmol) and $\text{Zn}(\text{OAc})_2 \cdot 2\text{H}_2\text{O}$ (0.22g, 1.0 mmol) were added under stirring to pentan-1-ol (10 mL) in a 25 mL oneneck round-bottomed flask equipped with an air condenser. Then, a catalytic amount of DBU was added, and the mixture was stirred and heated at 135 °C under N_2 over 24 h. After cooling under N_2 , pentan-1-ol was removed under reduced pressure. The collected solid was purified by column chromatography with a mixture of CHCl_3 -MeOH (20:1) as eluents to afford 1a₁; yield: 0.68 g (53%). m.p. > 320°C. ^1H NMR (500 MHz, CDCl_3): δ = 7.340 (br s, 12 H, ArH), 7.044 (br s, 12 H, ArH), 3.452 (br s, 4H, 4CH), 2.300 (br s, 12H, 4ArCH₃), 1.394 (br s, 24 H, 4CH(CH₃)₂). MS (LDI-1700-TOF): m/z calcd for $[\text{M} + \text{H}^+]$: 1169.4; found: 1169.6 $[\text{M} + \text{H}^+]$. IR (KBr) 1247 cm^{-1} (C-O-C). Anal. Calcd for $\text{C}_{72}\text{H}_{64}\text{N}_8\text{O}_4\text{Zn}$ (1168.4): C, 73.87; H, 5.51; N, 9.57. Found: 72.85; H, 5.86; N, 9.43.

1b₁; yield 0.65 g (51%). m.p. > 320°C. MS (LDI-1700-TOF): m/z calcd for $[\text{M} + \text{H}^+]$: 1168.4; found: 1168.3 $[\text{M} + \text{H}^+]$. IR (KBr) 1248 cm^{-1} (C-O-C). Anal. Calcd for $\text{C}_{72}\text{H}_{64}\text{N}_8\text{O}_4\text{Cu}$ (1167.4): C, 73.98; H, 5.52; N, 9.59. Found: 72.64; H, 5.87; N, 9.24.

1c₁; yield: 0.56 g (49%). m.p. > 320°C. MS (LDI-1700-TOF): m/z calcd for $[\text{M} + \text{H}^+]$: 1163.4; found: 1163.9 $[\text{M} + \text{H}^+]$. IR (KBr) 1249 cm^{-1} (C-O-C). Anal. Calcd for $\text{C}_{72}\text{H}_{64}\text{N}_8\text{O}_4\text{Ni}$ (1162.4): C, 74.29; H, 5.54; N, 9.63. Found: 73.68; H, 5.73; N, 9.48.

1d₁; yield: 0.52 g (44%). m.p. > 320°C. MS (LDI-1700-TOF): m/z calcd for $[\text{M} + \text{H}^+]$: 1164.4; found: 1164.9 $[\text{M} + \text{H}^+]$. IR (KBr) 1248 cm^{-1} (C-O-C). Anal. Calcd for $\text{C}_{72}\text{H}_{64}\text{N}_8\text{O}_4\text{Co}$ (1163.4): C, 74.28; H, 5.54; N, 9.62. Found: 73.55; H, 5.76; N, 9.45.

1e₁; yield: 0.50 g (43%). m.p. > 320°C. MS (LDI-1700-TOF): m/z calcd for $[\text{M} + \text{H}^+]$: 1160.4; found: 1160.8 $[\text{M} + \text{H}^+]$. IR (KBr) 1246 cm^{-1} (C-O-C). Anal. Calcd for $\text{C}_{72}\text{H}_{64}\text{N}_8\text{O}_4\text{Mn}$ (1159.4): C, 74.53; H, 5.56; N, 9.66. Found: 73.66; H, 5.82; N, 9.45.

1a₂; yield: 0.64 g (50%). m.p. > 320°C. ^1H NMR (500 MHz, CDCl_3), δ = 7.359-7.469 (m, 12 H, ArH), 7.139-7.243 (m, 16 H, ArH), 1.361-1.555 (m, 36 H, 4t- C_4H_9). MS (LDI-1700-TOF): m/z calcd for $[\text{M} + \text{H}^+]$: 1169.4; found: 1169.0 $[\text{M} + \text{H}^+]$. IR (KBr) 1235 cm^{-1} (C-O-C). Anal. Calcd for $\text{C}_{72}\text{H}_{64}\text{N}_8\text{O}_4\text{Zn}$ (1168.4): C, 73.87; H, 5.51; N, 9.57. Found: 72.85; H, 5.86; N, 9.43.

1b₂; yield: 0.68 g (53%). m.p. > 320°C. MS (LDI-1700-TOF): m/z calcd for $[\text{M} + \text{H}^+]$: 1168.4; found: 1168.0 $[\text{M} + \text{H}^+]$. IR (KBr) 1238 cm^{-1} (C-O-C). Anal. Calcd for $\text{C}_{72}\text{H}_{64}\text{N}_8\text{O}_4\text{Cu}$ (1167.4): C, 73.98; H, 5.52; N, 9.59. Found: 72.64; H, 5.87; N, 9.24.

1c₂; yield: 0.58 g (50%). m.p. > 320°C. MS (LDI-1700-TOF): m/z calcd for $[\text{M} + \text{H}^+]$: 1163.4; found: 1163.9 $[\text{M} + \text{H}^+]$. IR (KBr) 1238 cm^{-1} (C-O-C). Anal. Calcd for $\text{C}_{72}\text{H}_{64}\text{N}_8\text{O}_4\text{Ni}$ (1162.4): C, 74.29; H, 5.54; N, 9.63. Found: 73.68; H, 5.73; N, 9.48.

*Id*₂; yield: 0.54 g (46%). m.p. > 320°C. MS (LDI-1700-TOF): *m/z* calcd for [M + H⁺]: 1164.4; found: 1164.8 [M + H⁺]. IR (KBr) 1238 cm⁻¹ (C-O-C). Anal. Calcd for C₇₂H₆₄N₈O₄Co (1163.4): C, 74.28; H, 5.54; N, 9.62. Found: 73.55; H, 5.76; N, 9.45.

*Ie*₂; yield: 0.50 g (43%). m.p. > 320°C. MS (LDI-1700-TOF): *m/z* calcd for [M + H⁺]: 1160.4; found: 1160.8 [M + H⁺]. IR (KBr) 1236 cm⁻¹ (C-O-C). Anal. Calcd for C₇₂H₆₄N₈O₄Mn (1159.4): C, 74.53; H, 5.56; N, 9.66. Found: 73.66; H, 5.82; N, 9.45.

*Ia*₃; yield: 0.68 g (59%). m.p. > 320°C. ¹H NMR (500 MHz, CDCl₃): δ = 10.24-7.43 (m, 24 H, ArH), 7.04-4.78 (m, 12 H, ArH). MS (LDI-1700-TOF): *m/z* calcd for [M + H⁺]: 1149.2; found: 1149.6 [M + H⁺]. IR (KBr) 1247 cm⁻¹ (C-O-C). Anal. Calcd for C₆₈H₃₆N₁₂O₄Zn (1148.2): C, 70.99; H, 3.15; N, 14.61. Found: 70.78; H, 3.25; N, 14.23.

*Ib*₃; yield: 0.58 g (51%). m.p. > 320°C. MS (LDI-1700-TOF): *m/z* calcd for [M + H⁺]: 1148.2; found: 1148.1 [M + H⁺]. IR (KBr) 1248 cm⁻¹ (C-O-C). Anal. Calcd for C₆₈H₃₆N₁₂O₄Cu (1147.2): C, 70.10; H, 3.16; N, 14.63. Found: 69.89; H, 3.33; N, 14.46.

*Ic*₃; yield: 0.55 g (48%). m.p. > 320°C. MS (LDI-1700-TOF): *m/z* calcd for [M + H⁺]: 1143.2; found: 1143.5 [M + H⁺]. IR (KBr) 1248 cm⁻¹ (C-O-C). Anal. Calcd for C₆₈H₃₆N₁₂O₄Ni (1142.2): C, 71.41; H, 3.17; N, 14.70. Found: 71.51; H, 3.36; N, 14.45.

*Id*₃; yield: 0.60 g (53%). m.p. > 320°C. MS (LDI-1700-TOF): *m/z* calcd for [M + H⁺]: 1144.2; found: 1144.5 [M + H⁺]. IR (KBr) 1248 cm⁻¹ (C-O-C). Anal. Calcd for C₆₈H₃₆N₁₂O₄Co (1143.2): C, 71.39; H, 3.17; N, 14.69. Found: 71.63; H, 3.35; N, 14.43.

*Ie*₃; yield: 0.48 g (42%). m.p. > 320°C. MS (LDI-1700-TOF): *m/z* calcd for [M + H⁺]: 1140.2; found: 1140.4 [M + H⁺]. IR (KBr) 1247 cm⁻¹ (C-O-C). Anal. Calcd for C₆₈H₃₆N₁₂O₄Mn (1139.2): C, 71.64; H, 3.18; N, 14.74. Found: 71.83; H, 3.35; N, 14.57.

*Ia*₄; yield: 0.52 g (59%). m.p. > 320°C. ¹H NMR (500MHz, CDCl₃): δ = 7.714-7.301 (m, 4 H, ArH), 7.181-6.257 (m, 8 H, ArH), 3.409 (m, 12 H, 4OCH₃), 3.190 (m, 16 H, 4OCH₂CH₂O). MS (LDI-1700-TOF): *m/z* calcd for [M + H⁺]: 873.2; found: 873.2 [M + H⁺]. IR (KBr) 1240 cm⁻¹ (C-O-C). Anal. Calcd for C₄₄H₄₀N₁₂O₄Zn (872.2): C, 60.45; H, 4.61; N, 12.82. Found: 61.05; H, 4.63; N, 12.85.

*Ib*₄; yield: 0.56 g (44%). m.p. > 320°C. MS (LDI-1700-TOF): *m/z* calcd for [M + H⁺]: 872.2; found: 872.4 [M + H⁺]. IR (KBr) 1241 cm⁻¹ (C-O-C). Anal. Calcd for C₄₄H₄₀N₁₂O₄Cu (871.2): C, 60.58; H, 4.62; N, 12.84. Found: 60.29; H, 4.47; N, 12.26.

*Ic*₄; yield: 0.44 g (35%). m.p. > 320°C. MS (LDI-1700-TOF): *m/z* calcd for [M + H⁺]: 867.2; found: 866.8 [M + H⁺]. IR (KBr) 1244 cm⁻¹ (C-O-C). Anal. Calcd for C₄₄H₄₀N₁₂O₄Ni (866.2): C, 60.92; H, 4.65; N, 12.92. Found: 60.69; H, 4.48; N, 12.60.

*Id*₄; yield: 0.48 g (38%). m.p. > 320°C. MS (LDI-1700-TOF): *m/z* calcd for [M + H⁺]: 868.7; found: 868.8 [M + H⁺]. IR (KBr) 1242 cm⁻¹ (C-O-C). Anal. Calcd for C₄₄H₄₀N₁₂O₄Co (867.2): C, 60.90; H, 4.65; N, 12.91. Found: 60.89; H, 4.57; N, 12.83.

*Ie*₄; yield: 0.47 g (38%). m.p. > 320°C. MS (LDI-1700-TOF): *m/z* calcd for [M + H⁺]: 864.2; found: 864.8 [M + H⁺]. IR (KBr) 1245 cm⁻¹ (C-O-C). Anal. Calcd for C₄₄H₄₀N₁₂O₄Mn (867.2): C, 61.18; H, 4.67; N, 12.97. Found: 60.55; H, 4.92; N, 12.83.

*2a*₁; yield: 0.68 g (53%). m.p. > 320°C. ¹H NMR (500 MHz, CDCl₃): δ = 7.309-7.622 (m, 12 H, ArH), 6.912-7.065 (m, 12 H, ArH), 3.538 (br s, 4 H, 4CH), 2.145-2.227 (m, 12 H, 4ArCH₃), 1.187-1.340 (m, 24 H, 4CH(CH₃)₂). MS (LDI-1700-TOF): *m/z* calcd for [M + H⁺]: 1169.4; found: 1169.0 [M + H⁺]. IR (KBr) 1251 cm⁻¹ (C-O-C). Anal. Calcd for C₇₂H₆₄N₈O₄Zn (1168.4): C, 73.87; H, 5.51; N, 9.57. Found: 72.95; H, 5.66; N, 9.53.

$2b_1$; yield: 0.65 g (51%). m.p. > 320°C. MS (LDI-1700-TOF): m/z calcd for $[M + H]^+$: 1168.4; found: 1168.0 $[M + H]^+$. IR (KBr) 1252 cm^{-1} (C-O-C). Anal. Calcd for $\text{C}_{72}\text{H}_{64}\text{N}_8\text{O}_4\text{Zn}$ (1168.4): C, 73.98; H, 5.52; N, 9.59. Found: 72.64; H, 5.87; N, 9.24.

$2a_2$; yield: 0.64 g (50%). m.p. > 320°C. $^1\text{H NMR}$ (500 MHz, CDCl_3), δ = 7.305-7.389 (m, 12 H, ArH), 6.857-7.031 (m, 16 H, ArH), 1.290-1.347 (m, 36 H, 4t- C_4H_9). MS (LDI-1700-TOF): m/z calcd for $[M + H]^+$: 1169.4; found: 1169.0 $[M + H]^+$. IR (KBr) 1251 cm^{-1} (C-O-C). Anal. Calcd for $\text{C}_{72}\text{H}_{64}\text{N}_8\text{O}_4\text{Zn}$ (1168.4): C, 73.87; H, 5.51; N, 9.57. Found: 72.85; H, 5.86; N, 9.43.

$2b_2$; yield: 0.68 g (53%). m.p. > 320°C. MS (LDI-1700-TOF): m/z calcd for $[M + H]^+$: 1168.4; found: 1168.0 $[M + H]^+$. IR (KBr) 1253 cm^{-1} (C-O-C). Anal. Calcd for $\text{C}_{72}\text{H}_{64}\text{N}_8\text{O}_4\text{Cu}$ (1167.4): C, 73.98; H, 5.52; N, 9.59. Found: 72.64; H, 5.87; N, 9.24.

3. RESULTS AND DISCUSSION

3.1. Synthesis and Characterization

According to literature [16], a modified method was used to synthesize twenty-four Pc compounds $1a_1\sim 1e_4$ and $2a_1\sim 2b_2$ in two steps from 4-nitro-phthalonitrile or 3-nitro-phthalonitrile. The synthetic route involves the aromatic nucleophilic substitution reaction between nitro-phthalonitriles and a suitable oxygen nucleophile followed by cyclotetramerization of the resultant phthalonitrile derivatives. First, we chose two kinds of nitro-phthalonitriles and four kinds of oxygen nucleophiles as starting materials to synthesize phthalonitrile derivatives with good yield in the presence of LiOH and anhydrous DMSO at room temperature. Upon treatment with inorganic salts in refluxing pentan-1-ol with DBU as catalyst under nitrogen, MPcs $1a_1\sim 1e_4$ and $2a_1\sim 2b_2$ were synthesized from the aforementioned phthalonitrile derivatives, which could be purified by column chromatography. Their synthesized route and molecular structures were displayed in Figure 1.

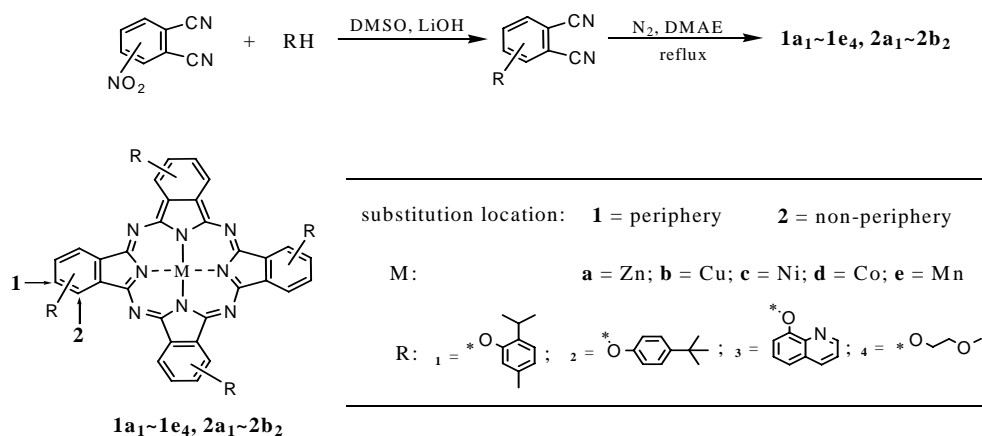


Figure 1. Synthesis and molecular structures of $1a_1\sim 1e_4$ and $2a_1\sim 2b_2$.

The obtained twenty-four Pc compounds were characterized by methods of ^1H NMR, TOF-MS, UV-vis, IR and elemental analysis (Section 2.3), which were consistent with the proposed structures. The ^1H NMR spectra of the Pc compounds without zinc were precluded for that the paramagnetic nature of them in a square planar environment, which phenomenon can be seen in our previous investigations [21].

3.2. Solubility and Stability of $1a_1\sim 1e_4$ and $2a_1\sim 2b_2$

The Pcs $1a_1\sim 1e_4$ and $2a_1\sim 2b_2$, all presented excellent solubility in CHCl_3 , CH_2Cl_2 , pyridine and quinoline (10^{-1} mol/L), but they were hardly soluble in acetone and methanol ($\leq 10^{-5}$ mol/L). Only the Pcs processing Zn, $1a_1\sim 1a_4$ and $2a_1\sim 2a_2$, could slightly dissolve in acetone (10^{-5} mol/L). The Pcs with Zn, Co and Mn, $1a(d,e)_1\sim 1a(d,e)_4$ and $2a_1\sim 2a_2$, could dissolve in DMF and DMSO (10^{-1} mol/L), but in which the solubility of Pcs with another two metals Cu and Ni, $1b(c)_1\sim 1b(c)_4$ and $2b_1\sim 2b_2$, was poor ($< 10^{-5}$ mol/L). The good solubility facilitated the structural characterization and property investigation of them.

However, the stability of them in solution was not as good as in solid state. It was found that they could be quickly degraded by sunlight in HCCl_3 , especially $1a_1\sim 1a_4$ and $2a_1\sim 2a_2$. The color of their solutions converted from blue-green to slight yellow under midday sunlight for 30 min, and accordingly the UV-vis spectra occurred obvious change, e.g. the UV-vis spectrum of $1a_4$ in chloroform (Figure 2). The solutions of $1b_1\sim 1b_4$ and $2b_1\sim 2b_2$ in chloroform displayed color change after two days, and the solutions of other Pcs in chloroform didn't occur remarkable color difference even if one week had past. According to the views of the literatures [22,23], the poor stability of their solutions might be ascribed to the photocatalysis of Pcs containing non-transition metals, especially Zn (II), which monomer in solution is efficient photocatalyst for phenols and itself. As a photosensitizer, it is excited to its triplet state, and then transfers the energy to ground-state triplet oxygen O_2 ($^3\Sigma_g$) forming the excited-state singlet oxygen, O_2 ($^1\Delta_g$), through the so called Type II mechanism. The aforementioned photodegrade of $1a_4$ in solution occurs via attack by singlet oxygen generated by it.

3.3. Impact of Metals on UV-vis Spectra

The UV-vis spectral data of twenty-four Pcs $1a_1\sim 1e_4$ and $2a_1\sim 2b_2$ were given in Table 1, from which the impact of metals, substituents and substitution positions on the UV-vis spectra of them could be seen clearly. When the substituent and the substitution position of Pcs were same, the coordinated metals in the center of Pc ring caused an uneven red-shifted impact on the Q bands and followed an order: $\text{Mn} > \text{Zn} \approx \text{Cu} > \text{Ni} \approx \text{Co}$. The Q band wavelength of the Pcs with Zn (Ni) and the Pcs with Cu (Co) are almost equal, and the Q band wavelength of the Pcs with Zn (Cu) red shifted no more than 10 nm comparing with that of the Pcs with Ni (Co). But the Q bands of the Pcs with Mn red shifted approximate 50 nm relative to that of the Pcs with other metals. The phenomenon could also be clearly showed in the UV-vis spectra of $1a_1\sim 1e_1$ (Figure 3). To refer to the previously reported results [21,24,25], the Q band difference of the Pcs with Co, Ni, Cu and Zn derived from different d electron number in the several metals. The reason that the Q band of Pcs with Mn markedly

shifted 50 nm towards red region relative to the others, should be that there is a Mn^{III} , not Mn^{II} , in the center of Pc ring like the common manganese Pc complexes [26,27]. Moreover, comparing with the Pc compounds with common M^{II} , the distinctly higher B bands and the additional bands near 520 nm in the UV-vis were also the characters of Pc compounds with Mn^{III} (e.g. $1e_1\sim 1e_4$ Figure 3) [28]. This implied that it might be a way to cause the Q band to shift largely by altering the value of center metal.

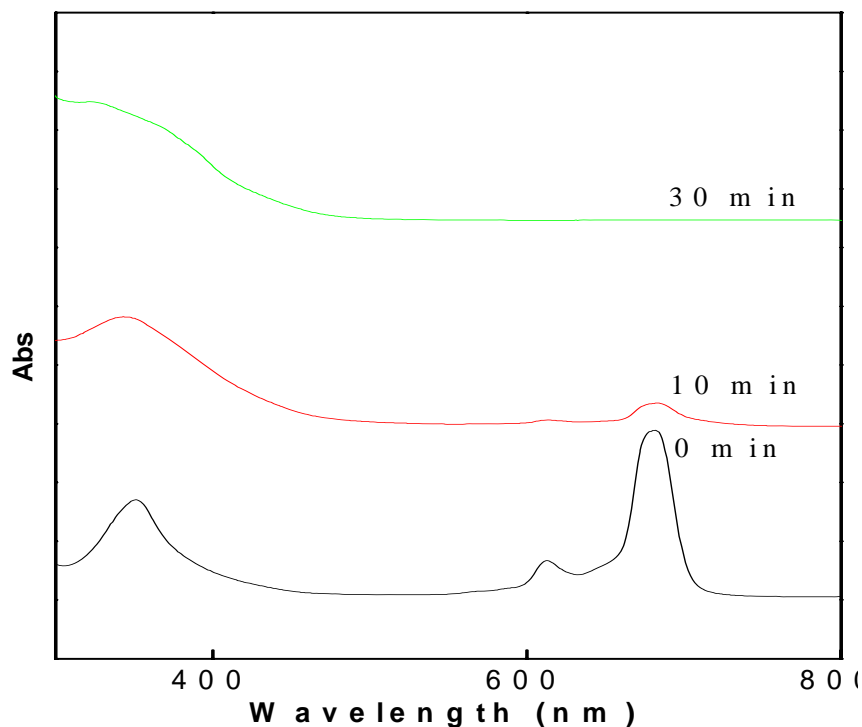


Figure 2. UV-vis spectral changes of MPc $1a_4$ in chloroform (2.0×10^{-4} mol/L) under midday sunlight for 0 min (1), 10 min (2) and 30 min (3): showing the poor stability of $1a_4$ in chloroform.

Table 1. Parameters on UV-Vis spectra of $1a_1\sim 1e_4$ and $2a_1\sim 2b_2$ in chloroform (2.0×10^{-4} mol/L)

Sample	λ (nm) / Q (B) band				
	Zn	Cu	Ni	Co	Mn
$1a_1\sim 1e_1$	684 (353)	684 (340)	675 (332)	676 (327)	737 (391)
$1a_2\sim 1e_2$	682 (352)	683 (340)	674 (331)	674 (325)	734 (390)
$1a_3\sim 1e_3$	682 (358)	681 (340)	674 (331)	673 (326)	733 (388)
$1a_4\sim 1e_4$	682 (351)	680 (338)	672 (328)	673 (326)	732 (388)
$2a_1\sim 2b_1$	705 (331)	707 (327)			
$2a_2\sim 2b_2$	702 (332)	703 (336)			

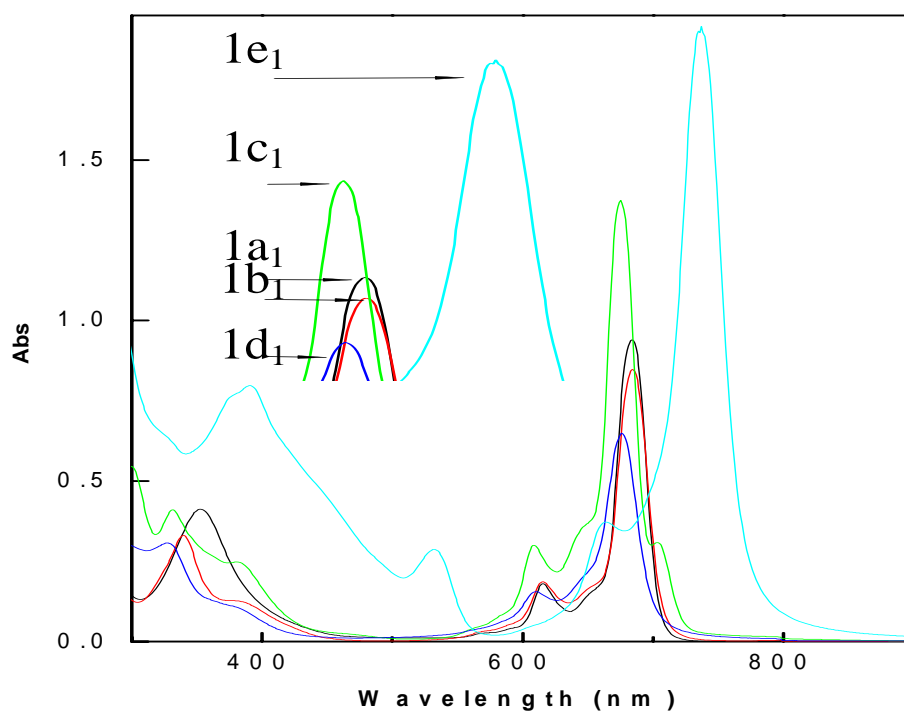


Figure 3. UV-vis spectra of $1a_1 \sim 1e_1$ in chloroform (2.0×10^{-4} mol/L): showing the impact of metals on Q bands.

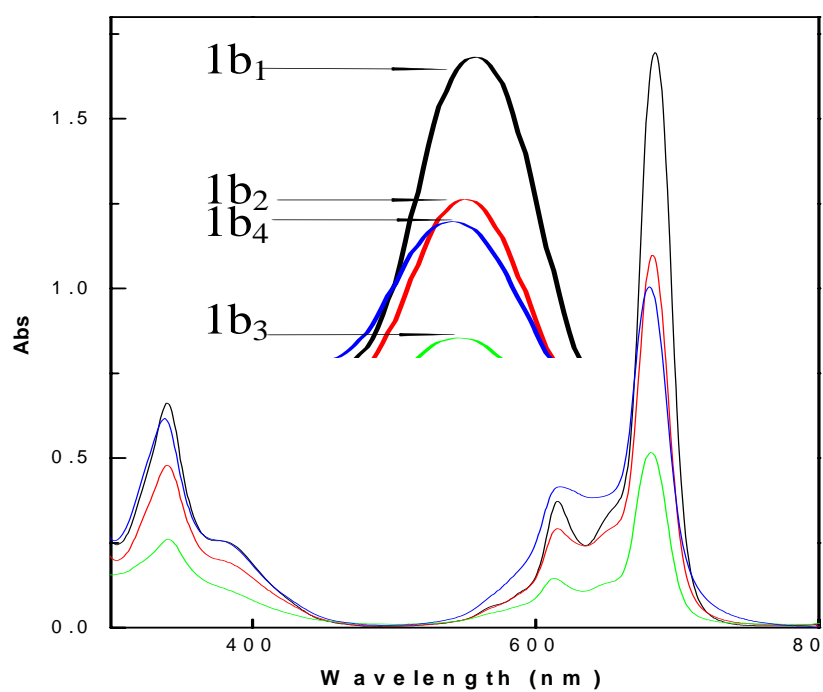


Figure 4. UV-vis spectra of $1b_1 \sim 1b_4$ in chloroform (2.0×10^{-4} mol/L): showing the impact of substituents on Q bands.

3.4. Impact of Substituents on UV-vis Spectra

When the metal and the substitution position of Pcs were uniform, from table 1 it is found that the impact of four substituents on the red shift of Q band followed a tendency: 2-isopropyl-5-methylphenoxy \geq 4-tert-butylphenoxy \geq quinolin-8-yloxy \geq 2-methoxyethoxy. But the difference is not great. Comparing one substituent with its neighboring one in the above order, the gaps between the two Q bands of the two corresponding Pcs were no more than 2 nm. This might be attributed to that the atoms bonding directly with Pc ring all were oxygen in the four substituents and the other part of four substituents had less distinction in terms of pushing or pulling electrons. Here, the tendency of Q band depending on substituents could be directly indicated by the UV-vis spectra, e.g. that of $1b_1 \sim 1b_4$ (Figure 4). It suggested that the shift of Q band wouldn't be obvious if the atoms banding directly with Pc ring were same and their chemical circumstances were similar in different substituents. Namely, it must be change the atom banding directly with Pc ring or its chemical circumstance in substituent if a large Q band shift is demanded.

3.5. Impact of Substitution Positions on UV-vis Spectra

When the Pcs had same metal and substituent, from table 1 it was found that the substitution positions (periphery and non-periphery) gave a large impact on the Q bands of Pcs, which was non-periphery $>$ periphery. The Q band of non-peripherally substituted Pcs red shifted more than 20 nm relative to that of peripherally substituted Pcs, which could be seen in their UV-vis spectra, e.g. that of $1a_2$ and $2a_2$ (Figure 5). According to our previous investigation [20], the substituent at the non-peripheral substitution position of Pc ring help to enlarge the conjugate structure of Pc ring. The enlarged conjugate area was in favor of electron cloud delocalizing from substituents to 18- π electron system of Pc ring, which could lead to a red shift of Q band [36,37]. This meant that the two substitution positions, non-periphery and periphery, could give a largely different impact on the Q band of substituted Pc compounds.

4. CONCLUSION

Twenty-four Pcs, $1a_1 \sim 1e_4$ and $2a_1 \sim 2b_2$, were synthesized in two steps from 4-nitro-phthalonitrile or 3-nitro-phthalonitrile. They had excellent solubility in some organic solvents, but poor stability in solution. Their UV-vis spectra showed that the coordinated metals (Zn^{II} , Cu^{II} , Co^{II} and Ni^{II}) with II value had not obvious differences in terms of the impact on the Q bands. Analogously, the four substituents around Pc ring also generated a little distinction. But the substituent on the non-peripheral position of Pc ring offered a great red shift of Q band comparing with that on the peripheral position. The impacts of three aspects on the Q bands were concisely described as follows: $Mn > Zn \approx Cu > Ni \approx Co$; 2-isopropyl-5-methylphenoxy $>$ 4-tert-butylphenoxy $>$ quinolin-8-yloxy $>$ 2-methoxyethoxy; non-periphery $>$ periphery. The alternative ways to cause the Q band of Pc to have a big change were to alter the chemical value of metal in the center of Pc ring, replace the atom banding

directly with Pc ring or its chemical circumstance, and change the substitution position of substituent on Pc ring (periphery or non-periphery).

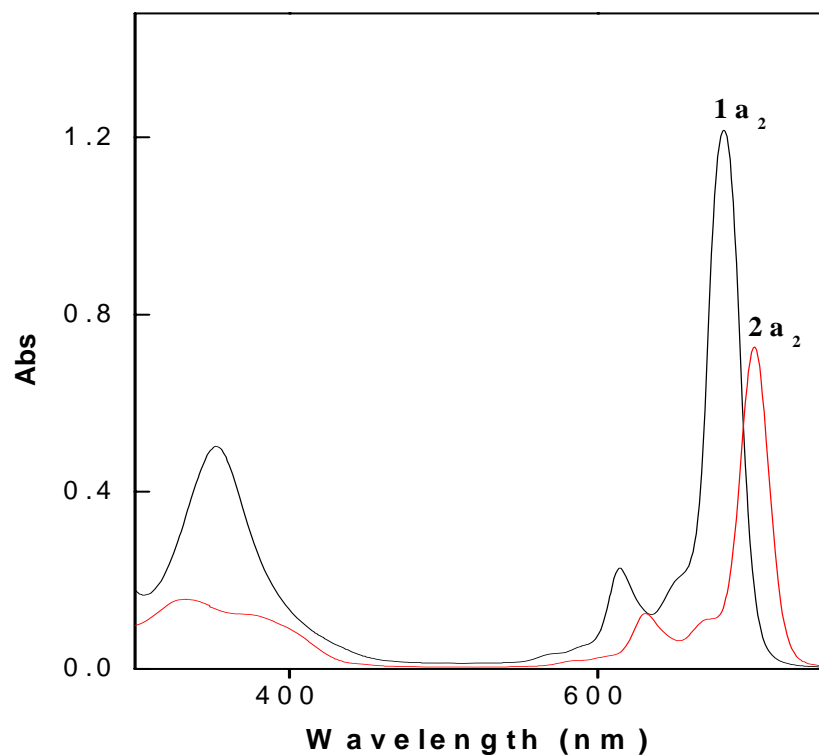


Figure 5. UV-vis spectra of $1a_2$ and $2a_2$ in chloroform (2.0×10^{-4} mol/L): showing the impact of substitution positions on Q bands.

ACKNOWLEDGEMENTS

Financial support of this project was provided by National Science Foundation of China (NSFC 20472014) and Jiang Su Science Foundation of China (JSSFC BK2005126). This project was supported by the 41th China Postdoctoral Science Foundation.

REFERENCES

- [1] N. Kobayashi, *Coordin. Chem. Rev.* 219-221 (2001) 99-123.
- [2] S. Griveau, J. Pavez, J.H. Zagal, F. Bedioui, *J. Electroanal. Chem.* 497 (2001) 75-83.
- [3] M.F. Joseph, J.K. Thomas, V.E. Sven, V. Thierry, K. Martti, P. André, T. Tienthong, K. Todd, B. Louis, *J. Am. Chem. Soc.* 121 (1999) 3453-3459.
- [4] C. Fabris, G. Jori, F. Giuntini, G. Roncucci, *J. Photoch. Photobiol. B* 64 (2001) 1-7.
- [5] M.P. Srinivasan, Y. Gu, R. Begum, *Colloid. Surf. A* 198-200 (2002) 527-534.
- [6] G. Liu, A. Klein, A. Thissen, W. Jaegermann, *Surf. Sci.* 539 (2003) 37-48.

- [7] J.H. Burroughes, C.A. Jones, R.H. Friend, *Nature* 335 (1998) 137-139.
- [8] N.B. McKeown, *Phthalocyanine Materials—Synthesis, Structure and Function*, Cambridge University Press, Cambridge, 1998.
- [9] P.M. Burnham, M.J. Cook, L.A. Gerrard, M.J. Heeney, D.L. Hughes, *Chem. Commun.* (2003) 2064-2065.
- [10] N. Ishikawa, Y. Kaizu, *Coordin. Chem. Rev.* 226 (2002) 93-101.
- [11] H. Kantekin, M. Rakap, Y. Gök, H.Z. Şahinbas, *Dyes Pigments* 74 (2007) 21-25.
- [12] C. Rager, G. Schmid, M. Hanack, *Chem. Eur. J.* 5 (1999) 280-288.
- [13] J. Rusanova, M. Pilkington, S. Decurtins, *Chem. Commun.* (2002) 2236-2237.
- [14] M. Brewis, N.B. McKeown, *Chem. Eur. J.* 4 (1998) 1633-1640.
- [15] M. Hanack, A. Beck, H. Lehmann, *Synthesis-Stuttgart.* (1987) 703-705.
- [16] C. Ma, D. Tian, X. Hou, Y. Chang, F. Cong, H. Yu, X. Du, G. Du, *Synthesis-Stuttgart.* 5 (2005) 741-748.
- [17] C. Ma, G. Du, Y. Cao, S. Yu, C. Cheng, W. Jiang, Y. Chang, X. Wang, F. Cong, H. Yu, *Dyes Pigments* 72 (2007) 267-270.
- [18] C. Ma, K. Ye, S. Yu, G. Du, Y. Zhao, F. Cong, Y. Chang, W. Jiang, C. Cheng, Z. Fan, H. Yu, W. Li, *Dyes Pigments* 74 (2007) 141-147.
- [19] C.C. Leznoff, S.M. Marcuccio, S. Greenberg, A.B. P. Lever, K. B. Tomer, *Can. J. Chem.* 63 (1985) 623-632.
- [20] F.D. Cong, B. Ning, H.F. Yu, X.H. Cui, B. Chen, S.G. Cao, C.Yu. Ma, *Spectrochim. Acta Part A* 62 (2005) 394-397.
- [21] F.D. Cong, B. Ning, X.G. Du, C.Yu. Ma, H.F. Yu, B. Chen, *Dyes Pigments* 66 (2005) 149-154.
- [22] E. Marais, R. Klein, E. Antunes, T. Nyokong, *Journal of Molecular Catalysis A: Chemical* 261 (2007) 36-42.
- [23] A. Ogunsipe, T. Nyokong, *Journal of Molecular Structure* 689 (2004) 89-97.
- [24] K.R. Venugopala Reddy, J. Keshavayya, J. Seetharamappa, *Dyes Pigments* 59 (2003) 237-244.
- [25] S. Sasmaz, E. Agar, A. Agar, *Dyes Pigments* 42 (1999) 137-142.
- [26] C.C. Leznoff, L.S. Black, A. Hiebert, P.W. Causey, D. Christendat, A.B.P. Lever, *Inorg. Chim. Acta* 359 (2006) 2690-2699.
- [27] J. Obirai, T. Nyokong, *Electrochim. Acta* 50 (2005) 5427-5434.
- [28] M.J. Stillman, T. Nyokong, in: C.C. Leznoff, A.B.P. Lever (Eds.), *Phthalocyanines: Properties and Applications*, vol. 1, VCH, New York, 1989 (Chapter 3).
- [29] S. Qu, Y. Gao, C. Zhao, Y. Wang, S. Fu, Y. Song, D. Wang, J. Qiu, C. Zhu, *Chem. Phys. Lett.* 367 (2003) 767-770.
- [30] A. Grofcsik, P. Baranyai, I. Bitter, V. Csokai, M. Kubinyi, K. Szegletes, J. Tatai, T. Vido'czy, *J. Mol. Struct.* 704 (2004) 11-15.
- [31] M. Durmusx, T. Nyokong, *Tetrahedron* 63 (2007) 1385-1394.
- [32] D. Wróbel, A. Boguta, *J. Photoch. Photobio. A* 150 (2002) 67-76.
- [33] M. Durmusx, C. Lebrun, V. Ahsen, *J. Porphyr. Phthalocya.* 8 (2004) 1175-1186.
- [34] G. Cheng, X. Peng, G. Hao, V. O. Kennedy, I. N. Ivanov, K. Knappenberger, J. J. Hill, M. A. J. Rodgers, M. E. Kenney, *J. Phys. Chem. A* 107 (2003) 3503-3514.
- [35] M. Aoudia, G. Cheng, V. O. Kennedy, M. E. Kenney, M. A. J. Rodgers, *J. Am. Chem. Soc.* 119 (1997) 6029-6039.

-
- [36] K.P. Unnikrishnan, J. Thomas, V.P.N.Nampoori, C.P.G. Vallabhan, *Synth. Met.* 139 (2003) 371-375.
- [37] S.N. Hari, H. Michael, P. Georg, K.E. Michael, *Chem. Phys.* 245 (1999) 17-26.

